

The Wilberforce pendulum: a complete analysis through RTL and modelling



Introduction

The Wilberforce [1] pendulum is a didactical device often used in class demonstration to show the amazing phenomenon of coupled oscillations (rotational and longitudinal) producing beats in a special mass-spring set up. The phenomenon is particularly surprising for a *distant* observer who easily detects the longitudinal motion but may skip the presence of rotation. To him (her) the vertical oscillation appear to damp out completely and then it rises again without external action (as if an invisible force would come in). In this contribution we propose a revised version of the classical experiment, as an example of an efficient didactical use of modern technologies, suggesting a deeper understanding of phenomena through real time data acquisition and advanced computer modelling.

Our experimental set up



This device picked up the curiosity of many [2] , among which Arnold Sommerfeld, who gave us a complete theoretical treatment [3] . Recently it was studied also with the aid of an RTL system (sonar interfaced to a PC) by measuring the vertical oscillation [4]. Nobody, however, completely characterized the Wilberforce pendulum motion with RTL (both longitudinal and rotational coupled oscillations). In this contribution we show how it may be done by using, besides the sonar, also a Non-Contact Rotation Sensor [5] (NCRS).

Our NCRS is an optical probe that exploits the intensity modulation of a polarized light beam (emitted by a LED placed behind a rotating Polaroid driven by a motor). The light beam, after a reflection by a second Polaroid attached to the rotating target, is detected by a photodiode. A lock-in technique and some more electronics gives an output voltage that is linearly proportional to the rotation angle.

The pendulum is produced by LABTREK [6] with an helicoidal spring and a cylindrical brass mass of about 0.5 kg. The upper end of the spring is blocked to a rigid holder, and the cylinder is blocked to the lower end of the spring. A reflector screwed to the lower cylindrical end is covered by a Polaroid disc.

Both the sonar and the NCRS are placed at ground (side by side) so that both the ultrasonic beam and the IR light beam reach the target reflector (the useful distance range is between 0.5 m and 1.0 m).

Experimental results

An example of the recorded rotation angle and of the vertical displacement obtained using a Personal Computer and the LabPro interface driven by LoggerPro [7]:

Fig. 1: The pendulum with NCRS and SONAR

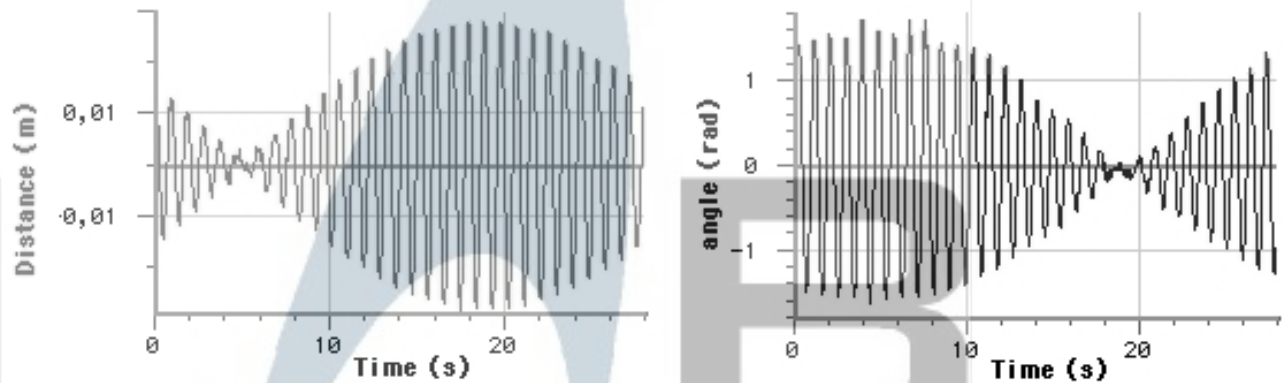


Fig. 2: Displacement and angle as functions of time

The beats in figure 2 are evident: the vertical oscillation slowly dumps out while rotational oscillation rises, then the process reverses (approximately every 1/2 minute) with the energy associated to each oscillation that transfers from one motion to the other, with negligible dissipation. The two oscillations must have the same period (in our case about 0.91 s) in order to achieve a complete energy exchange.

By plotting the angle as a function of displacement we see that the phase angle between the two signals covers a whole region in the phase space.

The total energy in each motion is made of an elastic potential term E_e and of a kinetic term [8] E_k .

For the longitudinal motion: $E_T = E_{kT} + E_{eT} = (m/2)v^2 + (k/2)z^2$ (where m is the mass, v the velocity, k the elastic constant, and z the displacement from the equilibrium position).

For the rotational motion: $E_R = E_{kR} + E_{eR} = (I/2)\omega^2 + (D/2)\alpha^2$ (where I is the inertial momentum, $\omega = d\alpha/dt$ the angular velocity, D the torsional constant and α the rotation angle).

The “total pendulum energy” is therefore $E = E_T + E_R = (m/2)v^2 + (k/2)z^2 + (I/2)\omega^2 + (D/2)\alpha^2$.

In order to evaluate the behaviour of the various terms one must know the values of the four parameters m, k, I, D . To measure the mass m we only need a scale, or a calibrated force sensor. To calculate k we may measure the spring elongation under a known force (e.g. the cylinder weight mg). We may also calculate the inertial momentum I for a simple geometry [9]: for a cylinder of radius R and mass m it is $I = mR^2/2$. The torsion constant D may be calculated from the measured period $T = 2\pi/\omega$ and the relation that gives the angular velocity: $\omega^2 = D/I$, or $D = I(2\pi/T)^2$.

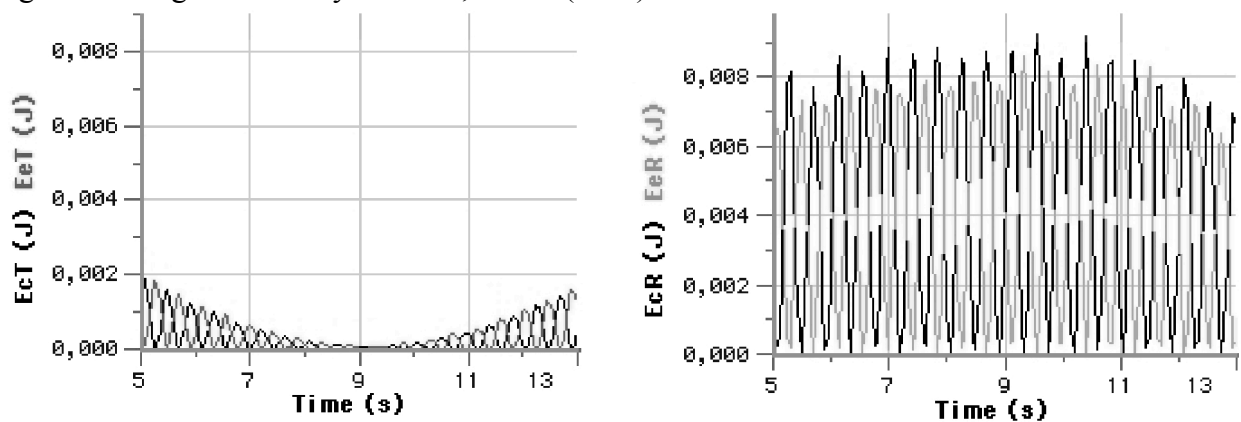


Fig. 3: Elastic and kinetic energies for longitudinal (E_{eT} , E_{cT}) and rotational (E_{eR} , E_{cR}) motions

The time evolution of elastic and kinetic energies may be calculated from the measured angles and displacements, as shown in figure 3 .

By adding elastic and kinetic terms we obtain the “total energy for each motion” (figure 4).

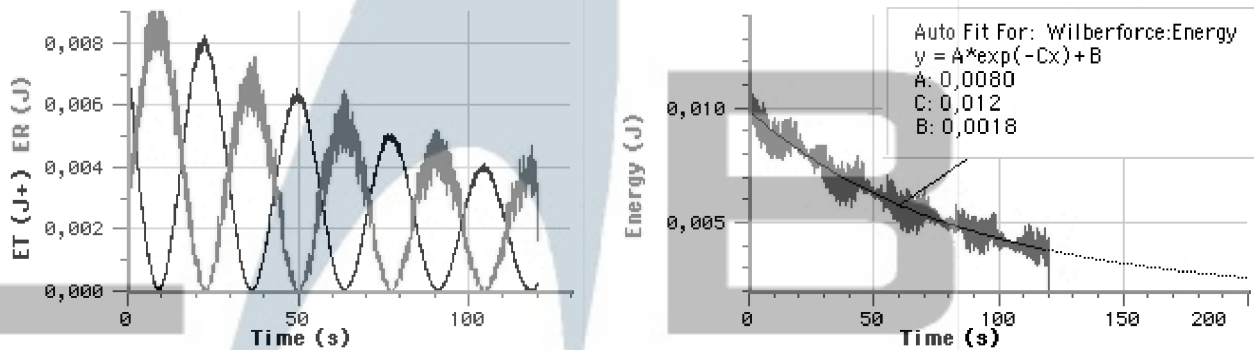


Figure 4: Translational (ET), rotational (ER) energies and their sum as functions of time

By finally adding the two “pulsed” terms $ET(t)$ and $ER(t)$ we obtain the total energy that appears to decrease very slowly in time (in figure 4 we see that the time constant of the exponential decay is about 170 s). The oscillations that modulate the exponential decay, at this stage of our investigation, may be attributed to “noise” or to approximation in the parameters’ values used to calculate the total energy. We will see later that there is a different explanation ...

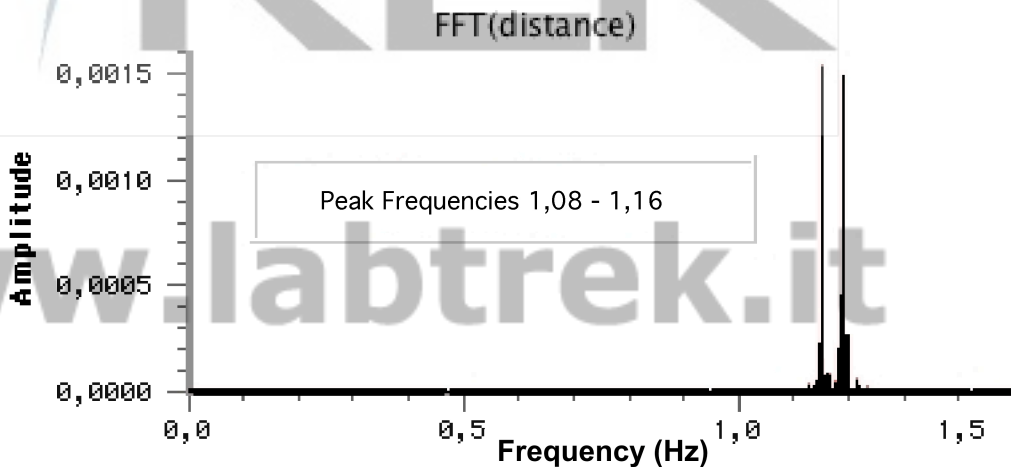


Fig. 5: Fourier Transform plot (two frequencies appear)

Even if at first sight the two oscillations appear to have exactly the same frequency, a Fourier analysis (either of the longitudinal or of the rotational motion) shows that two frequencies are present (figure 5): this is due to the coupling between two normal modes that can be excited by properly choosing the initial conditions, as can be better shown by using a simulation.

We may build a simulation of the whole process by using recursive numerical computation, either exploiting the graphic calculator tools for differential calculus, or on a PC using software applications like Stella (or MathLab or Mathematica).

We write a set of differential equations for the coupled oscillators, accounting for a finite coupling constant $[10]\epsilon$ between rotation and displacement [11].

For longitudinal motion the main restoring force is $-kz$, but accounting for a *coupling* with rotational motion we add the term $-\epsilon\alpha$: the longitudinal acceleration is therefore $d^2z/dt^2 = -(kz + \epsilon\alpha)/m$.

For rotational motion the main restoring torque is $-D\alpha$, but accounting for a coupling with longitudinal motion we must add a term $-\epsilon z$: the angular acceleration is therefore $d^2\alpha/dt^2 = -(D\alpha + \epsilon z)/I$.

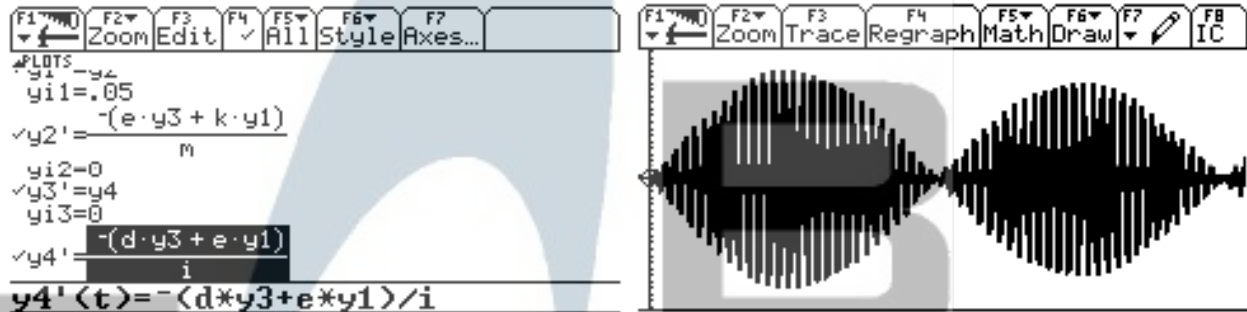


Fig. 6: Simulation obtained with a TI graphic calculator

This pair of equations may be solved, as shown in figure 6, using a TI-Voyage200 graphic calculator (with the parameters derived from experimental data and a properly chosen value for the coupling constant ϵ). The value of the coupling constant may also be evaluated through a detailed analysis of the system and by knowing details [12] of the spring (where the coupling takes place), but the simulation brings-in a great help: the ϵ value determines the beats period. The stronger is the coupling the faster becomes the energy transfer across modes, the shorter becomes the beating period.

Working with graphic calculators may be amusing and appealing (due to their great portability) but for such complex computations they may become extremely slow...

For didactical purpose it is better to switch to a PC-based application: we choose Stella (which joins power to easiness of use) to work out the simulation shown in figure 9 for displacement, angle, phase and energies respectively.

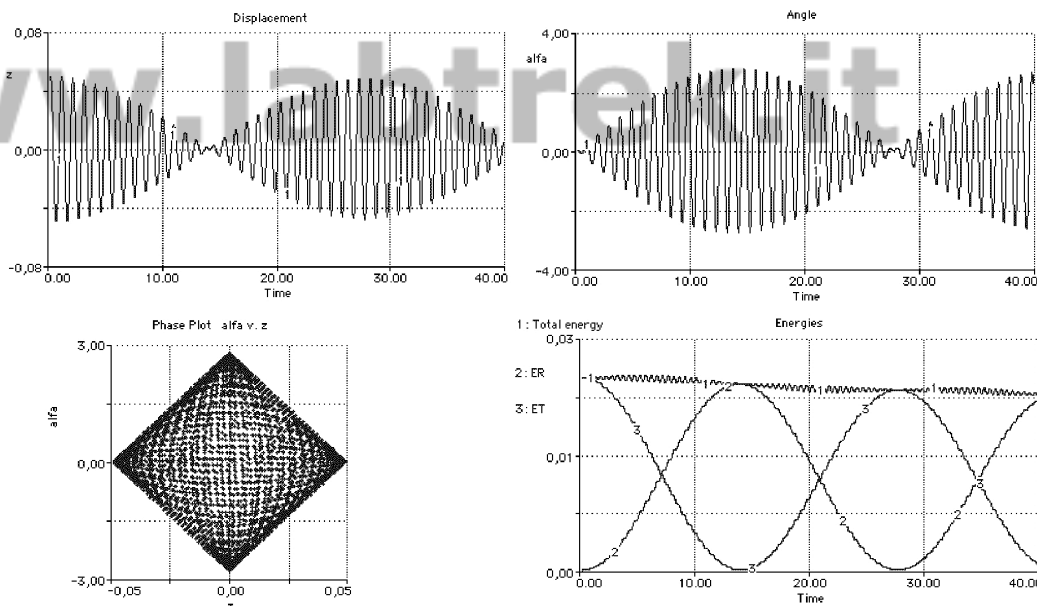


Fig. 7: Simulated displacement and angle vs. time ($z_0=5$ cm and $\alpha_0=0$ rad)

Figure 7 shows well the beating effect as well as the behaviour of the phase evolution. The last plot shows how the energy is exchanged between rotational and longitudinal oscillations, while total energy slowly decays due to dissipation.

One advantage of Stella is the easiness in setting the initial conditions, which are quite important in coupled oscillators. All the above results are in fact related to special initial conditions (zero for all velocities and for initial *angle*, and finite initial displacement). This is what usually happens when we start playing with the Wilberforce pendulum.

However if we choose different values (Fig. 8) we soon realize that the pendulum behaviour does sensibly change: for particular values of initial angle and displacement we may completely separate the two modes (in the sense that the energy stays substantially constant *for each mode*, and beating disappears).

Here we distinguish between *oscillation type* and *fundamental mode*. A fundamental mode is made of both of longitudinal and of rotational oscillations: there are two modes, one where angle and displacement are *in phase* and the other where they are *in phase opposition*. The two frequencies we detected experimentally are related to these two modes, which can be excited separately by a proper choice of initial conditions.

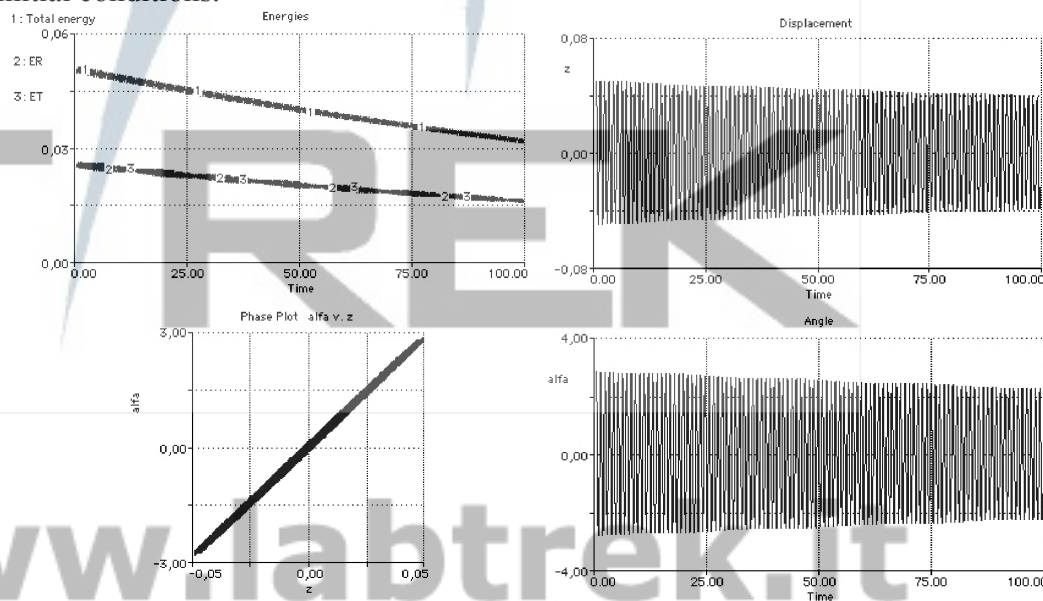


Fig. 8: Simulated behaviour with $z_0=5$ cm and $\alpha_0=2.85$ rad

Also dissipation is easily handled through Stella: both in figure 7 and 8 the simulations account for viscous forces (both in rotational and in longitudinal motion). In figure 8 the initial conditions are set to reach a complete mode decoupling (i.e. we excite a *single mode*), and the graph of the energies (rotational, translational and their sum) as a function of time shows that with these initial conditions no energy is transferred from rotation to translation or viceversa, and both amplitudes decrease smoothly in time. The phase plot shows that angle and displacement are now constantly in-phase. By reversing the initial angle we obtain the same behaviour, but with a constant dephasing of π . These two initial conditions are those that excite the *two decoupled oscillator modes* .

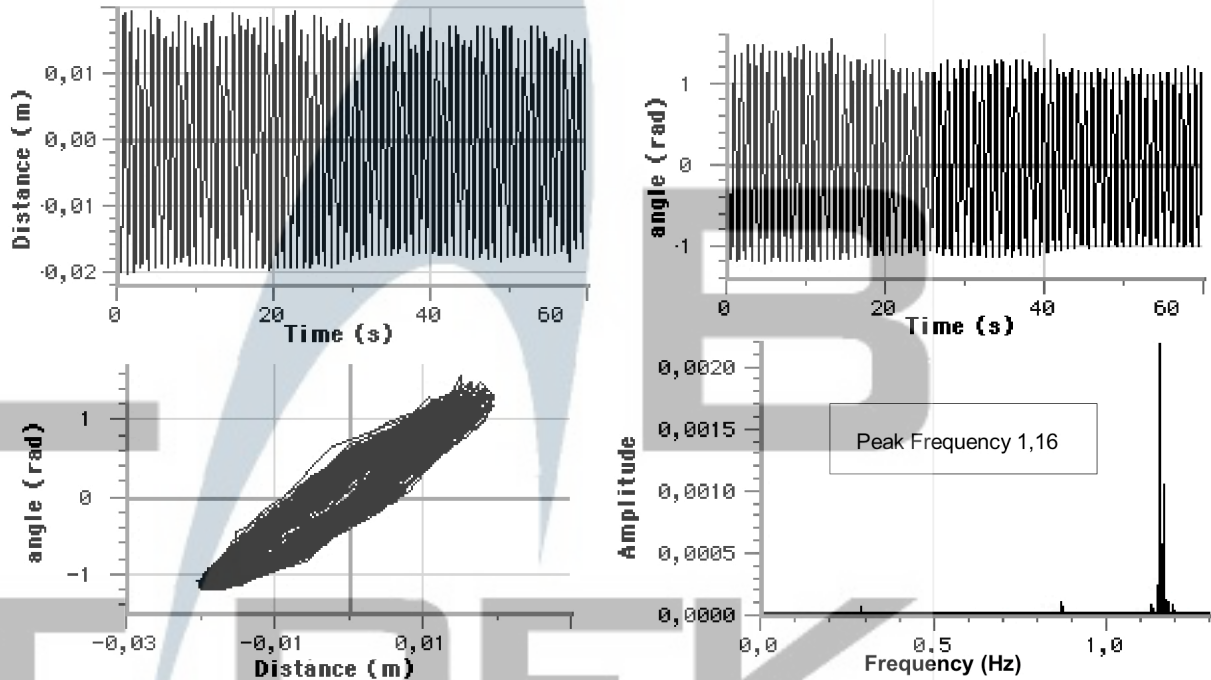


Fig. 9: Experimental behaviour with $z_0=2$ cm and $\alpha_0=1.14$ rad

A record of the actual oscillations, taken with these initial conditions, is reported in figure 9, where the FFT plot shows only one peak corresponding to the normal mode at higher frequency.

The slight oscillations that still appear in the simulated exponential decay of the total energy (in Figs. 7 and 8) tell us that something is missing in our model: because we introduced a coupling between modes we must also account for the energy associated to the coupling terms!

This is simply done by adding to the elastic and kinetic terms the coupling energy $E_c = \epsilon \alpha z$.

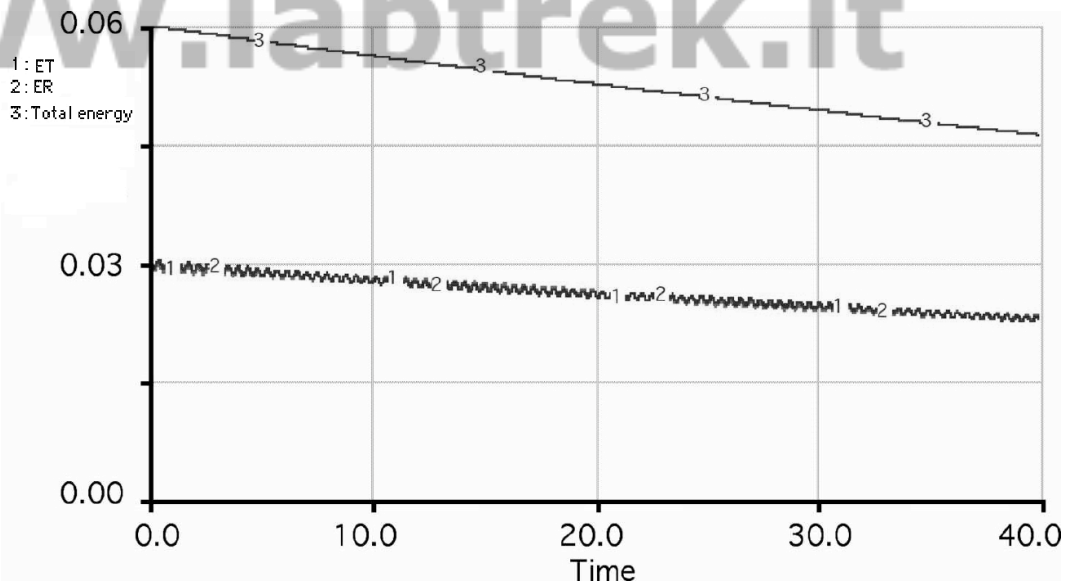


Fig 10 : Translational (1) , Rotational (2) and corrected Total (3) energy as functions of time

The results is shown in figure 10, where the oscillations (still visible in the energies associated to rotation and to displacement) disappear in the total energy curve.

It is easy to show how the beating frequency (that equals the difference between the two peaks observed in figure 5) depends on the value assigned to the coupling constant ϵ .

Also the simulation shows that, in presence of dissipation, a *unique* value of the ratio between the angular and the longitudinal friction coefficients may produce total decoupling of the two modes: any other value of this ratio will make impossible to produce pure oscillations *without* beatings!

In our experimental setup this matching was not perfect, leading to the slight residual mode coupling shown in Fig. 9.

References

1. Named after R.L. Wilberforce, a physics demonstrator at the Cavendish Labs, who in 1894 showed how a cylindrical mass suspended to an helicoidal spring may undergo both rotational and longitudinal oscillations, later publishing a paper on *Philosophical Magazine* **38**, 386 (1895).
2. U. Köpf: Wilberforce's pendulum revisited, *Am.J.Phys.* **58**, 833 (1990), R.E. Berg, T.S. Marshall: Wilberforce pendulum oscillations and normal modes, *Am.J.Phys.* **59**, 32 (1991), F.G.Karioris, Wilberforce pendulum, demonstration size: *The Phys. Teacher* **31**, 314 (1993).
3. A. Sommerfeld, *Mechanics of deformable bodies: lectures on theoretical physics II*, Academic, New York, 1964.
4. E. Debowska, S. Jakubowicz, Z. Mazur: Computer visualization of the beating of a Wilberforce pendulum *Eur. J. Phys.*, **20**, 89 (1999).
5. Made as prototype by Dusan Ponikvar (Ljubljana University), and summarized in *Rev. Sci. Instrum.* **70**, 2175 (1999).
6. <http://www.labtrek.it/>.
7. From Vernier Software <http://www.vernier.com>. Obviously similar interfaces and software, like those from PASCO or CMA, may be used as well.
8. It may be shown that in this system the gravitational potential energy may be excluded from the energy balance by an appropriate choice of the reference frame.
9. A more accurate measurement of the momentum of inertia I_x for a non-cylindrical mass may be obtained through a double measurement of the period: with the mass by alone and then by adding an annular cylinder of known mass and geometry (with well known value of inertial momentum I_n). The two measured periods obey to the relations $(T_1/2\pi)^2 = I_x/D$ $(T_2/2\pi)^2 = (I_x+I_n)/D$ giving: $(T_2/ T_1)^2=1+I_n/ I_x$, and finally $I_x= I_n T_1^2 / (T_2^2 - T_1^2)$.
10. See ref 2 and 3.
11. For example <http://www.phy.davidson.edu/StuHome/pecampbell/Wilberforce/Theory.htm>.
12. E.g. we must know the pitch of the spring turns and the Young modulus of the spring material.